Integration and Testing of Ice-/Mixed-Phase Precipitation Models for GPM Radar-Radiometer Algorithm Applications

William Olson[1], Kwo-Sen Kuo[2], Lin Tian[3], Mircea Grecu[3], Benjamin Johnson[4], Craig Pelissier[5], Andrew Heymsfield[6], Aaron Bansemer[6], and Stephen Munchak[7]

1: Joint Center for Earth Systems Technology/Univ. Maryland Baltimore County; 2: Earth System Science Interdisciplinary Center/Univ. Maryland College Park; 3: Goddard Earth Sciences Technology and Research/ Morgan State University; 4: Atmospheric and Environmental Research, Inc.; 5: Science Systems and Applications, Inc.; 6: National Center for Atmospheric Research; 7: NASA/Goddard Space Flight Center

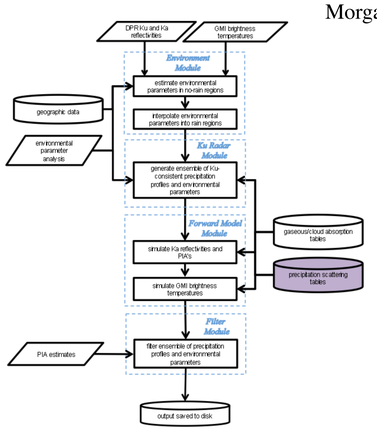

Why? **to improve the physical / statistical models used in GPM radar and combined radar-radiometer precipitation estimation algorithms.** At left is a schematic of the GPM combined radar-radiometer precipitation estimation algorithm. This algorithm uses input radar reflectivities from the Dual-frequency Precipitation Radar (DPR) and microwave radiances from the GPM Microwave Imager (GMI) to deduce profiles of precipitation in all phases (liquid, ice, and mixed-phase). The accuracy of these precipitation estimates depends not only on the validity of the input data, but also on the realism and representativeness of the physically-based precipitation profile models used to fit the input data.

In the figure at left, the microwave electromagnetic scattering properties of precipitation particles are tabulated in the purple static file. These tabulated scattering properties are functions of the assumed particle phase (temperature), size distribution, density distribution (for ice and mixed-phase), habit, and meltwater fraction. In addition to the tabulated scattering properties, for algorithm applications it is also important to prescribe the statistical behavior of precipitation particle size distributions; e.g., the covariance of particle size distribution parameters as a function of altitude. In sum, the objective of this work is to develop better parameterizations of the physical and statistical properties of ice and mixed-phase precipitation for algorithm applications.

Modeling of Ice-/Mixed-Phase Precipitation in Algorithms

The particle scattering models developed during the TRMM era assumed that all precipitation-sized particles were spherical, due to the simplicity of computing the single-scattering properties of spherical particles. However, it is known that larger raindrops are better approximated by oblate spheroids, and ice-phase precipitation particles exhibit a variety of complicated particle shapes. The focus of our investigation will be to see if we can find reasonable parameterizations of ice- and mixed-phase precipitation particle size distributions and particle shapes that produce bulk scattering properties which are consistent with simultaneous radar, radiometer, and *in situ* microphysics probe observations from the GPM field campaigns.

For each particle size in any prescribed particle size distribution, the mass (or density) of the particle, its shape or habit, and the meltwater fraction of the particle must be specified. Starting with purely ice-phase precipitation, we have examined the properties of both pristine crystals (plates, needles, dendrites) as well as aggregates of crystals. Aggregate ice particles are particularly important because they tend to be the dominant particle type among particles of relatively large size, and they also produce high radar reflectivities at the onset of melting.

We have implemented a 3-D growth model for pristine crystals and a pseudo-gravitational collection model to create aggregate particles. The figure at above right contains images of pristine ice crystals that were simulated using the growth model, and the various aggregates shown below the crystals are constructed from crystals of the same habit but with different sizes and spatial orientations, that have been sequentially collected. The constructed particles are filtered to represent different observed mass-size relations.

Using this method, roughly 6600 ice particles have been simulated, ranging from single pristine crystals to multi-crystal aggregates (sizes from 260 to 14,260 μm maximum dimension, although recently, particles greater than this maximum have been created). Each ice particle is constructed on a 3D numerical grid, and the microwave single-scattering properties of each particle are computed using the discrete dipole approximation (DDA; see Draine and Flatau, JOSA, 1994). In the DDA, a particle is represented by a grid of dipoles; each dipole interacts with an incoming electromagnetic wave as well as the scattered waves from all other dipoles in the particle. At above right are simulations of the single-scattering parameters of the individual particles (blue) using DDA, as well as the parameters for spheres of the same mass and either variable density (solid green) or a constant density of 0.1 g cm^{-3} (dashed green), derived from Mie theory.

Relative to the variable-density spheres, the constant density Mie spheres provide a better approximation to the aggregate particle backscatter efficiencies at 13.6 and 35.5 GHz. However, note that at the 89 and 165.5 GHz channel frequencies of the GMI, the asymmetry parameters of the Mie spheres are consistently higher than the aggregate asymmetry parameters. This characteristic leads to an inability of Mie spheres to simultaneously fit radar and high-frequency radiometer data in field campaign tests (see Olson et al., JAMC, 2016).

The properties of melting ice crystals, aggregates, and graupel are also being investigated. In one approach, the ice precipitation is represented on a 3D grid, and melting occurs based upon the exposure of ice to air (warming), while meltwater migrates toward local centers of mass to simulate the effects of surface tension. The evolution of a melting aggregate based upon this approach is shown at above right, with ice in blue and meltwater in red. The single-scattering properties of the melting aggregates are computed using DDA and "mapped" to spherical particles with the same mass and meltwater fraction in simplified 1D thermodynamic simulations of the melting layer. Simulations of bulk reflectivity and specific attenuation based upon polydispersions of melting particles are shown at right, for different initial median volume (liquid-equivalent) diameters. It is evident that polydispersions of melting homogeneous spheres (0.1 g cm^{-3}, solid lines) have properties that are different from those of melting nonspherical aggregates (dashed lines). The different attenuation-reflectivity relationships represented by these melting particles will impact combined radar-radiometer estimates of precipitation profiles.

simulated crystals/aggregates and their single-scattering properties

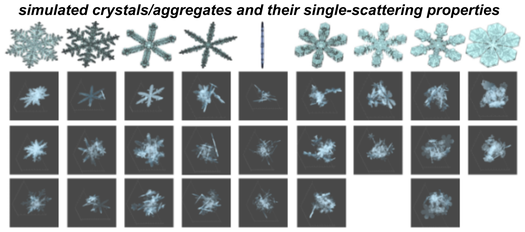

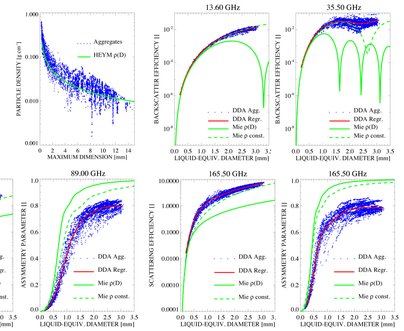

simulated melting aggregates

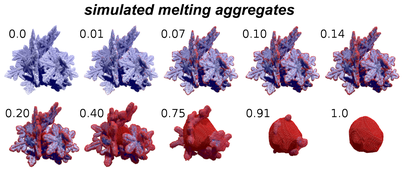

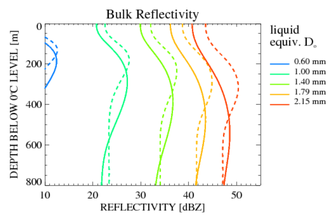

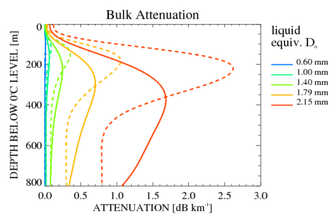

Scattering Properties of Large Aggregates

At right are recent calculations of the single scattering properties of nonspherical aggregate ice particles that extend the previous calculations from 3.1 mm liquid equivalent diameter to 5.0 liquid equivalent diameter. In terms of particle maximum dimension, this is an extension from 14 mm to 20 mm. The calculations were performed in a parallel computing environment using the discrete dipole approximation, and because of the large number of dipoles required to represent the particles, the domain decomposition MPI method of Numrich et al. (Proceedings of the *33rd Progress in Electromagnetics Research Symposium*, Taipei, Taiwan, 25-28 March, 2013) was utilized. The discrete dipole method was found to be in good agreement with invariant imbedding T-matrix calculations for various spheres, spheroids, and cylinders.

The red curves represent the locally-regressed values of extinction efficiency (top row), asymmetry parameter (middle row), and backscatter efficiency (bottom row), at 13.6 GHz (first column), 35.5 GHz (second column), 89 GHz (third column) and 165.5 GHz (fourth column). Mie scattering curves for different density assumptions are also plotted in green. Note that the asymmetry parameter of the nonspherical particles tends to "saturate" at the higher microwave frequencies for larger particle sizes but at lower values than any of the spherical models tested. Also, backscatter efficiencies tend to be high relative to those of the spherical particles.

Below are size-distribution-integrated scattering properties of nonspherical aggregate particles, including the radar reflectivity and asymmetry parameter.

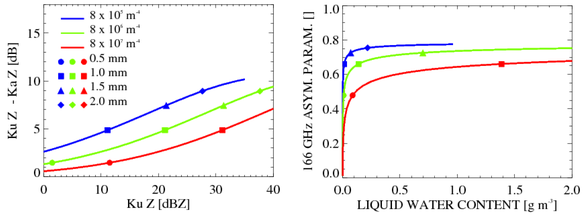

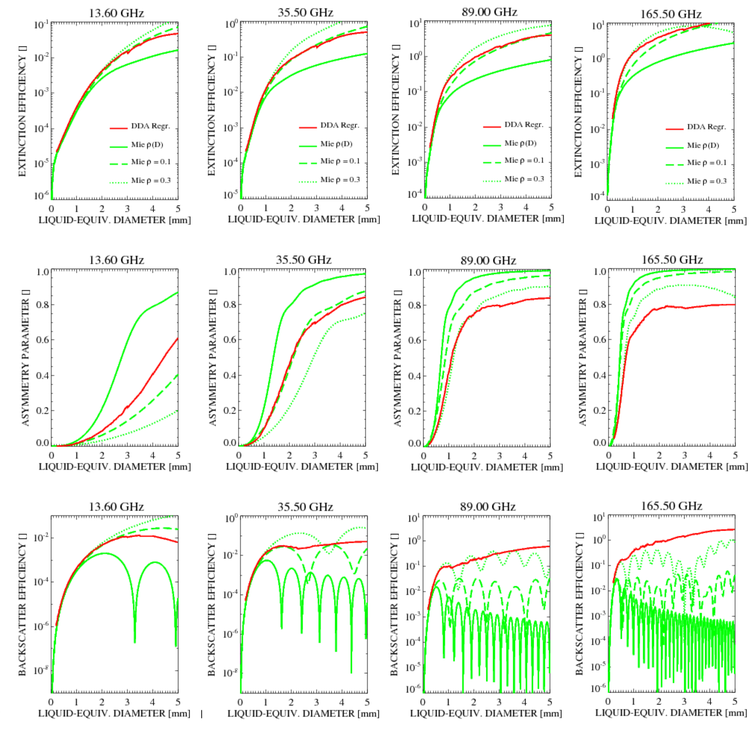

Consistency of Ice-/Mixed-Phase Particle Models with Field Data

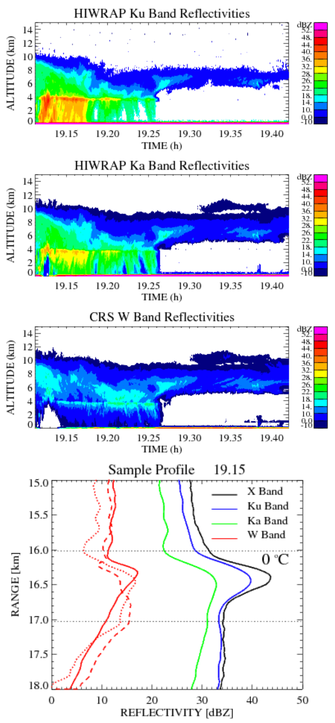

IPHEx During the Integrated Precipitation and Hydrology Experiment, four radars were deployed on the ER-2 aircraft. These included the X band ER-2 Doppler radar (EXRAD), operating at 9.6 GHz (X band), the High-Altitude Wind and Rain Airborne Profiler (HIWRAP), operating at 13.9 GHz (Ku band) and 33.7 GHz (Ka band), and the Cloud Radar System (CRS), operating at 94 GHz (W band). These radars were utilized to probe the structure of precipitation systems over North Carolina in May-June of 2014. We used these radar channels to discriminate between particle models in the melting layer, since the melting layer is relatively thin (generally < 1 km thickness), and radiometer observations do not necessarily detect much signal from changes in the melting layer. Also, the W band channel of CRS is sensitive to assumptions regarding particle shape, and therefore W band represents a kind of "bridge" to the higher-frequency radiometer channels.

In a preliminary study, the spherical and nonspherical particle models for both ice-phase and melting precipitation are utilized to estimate precipitation profiles using HIWRAP, and then the estimated profiles are used to simulate the W band reflectivities. The Ku and Ka band data from HIWRAP are closely fit by either spherical or nonspherical particle polydispersions using the estimation procedure, so the question is whether or not the coincident W band data can also be fit using the estimated precipitation profiles.

Shown in the panels at left are vertical cross-sections of HIWRAP Ku and Ka band radar reflectivities as well as the cross-section of CRS W band reflectivities from 3 May 2014 between 1900 and 1930 UTC. The solid curves at below left are the observed reflectivity profiles at 1909 UTC. The vertical profiles of Ku and Ka band reflectivities are used to estimate precipitation profiles based upon either the spherical (0.1 g cm^{-3}) ice/melting particles or the nonspherical aggregate ice/melting particles. The spherical particle estimated profile is used to simulate the W band attenuated reflectivity profile shown as the dotted red curve, while the nonspherical aggregate particle estimated profile is used to simulate the W band profile shown as the dashed red curve.

Note that above the freezing level, the nonspherical ice particle profile fits the W band data well, while the spherical ice particle profile does not, as expected from the Olson et al. (JAMC, 2016) study. On the other hand, both particle types only lead to rough fits of the observed W band profile in the melting layer and below. There are many factors that control the simulated radiative properties of the melting layer, such as the assumed densities/shapes of ice particles at the freezing level, the parameterization of the terminal fall speeds of the melting particles, and the effects of particle aggregation both above and within the melting layer. The fitting of the multi-channel radar data as a function of particle modeling assumptions will be explored by the team of investigators. In addition to the reflectivity data shown at left, Doppler velocities at each frequency are also available, as well as *in situ* particle microphysics probe observations. These observations will serve as additional constraints on the particle models.

GPM Ultimately, the bulk single-scattering properties of the simulated particle polydispersions developed in this study will be introduced into the GPM core mission combined radar-radiometer algorithm (through look-up tables) for further testing.